



European Research Council

Established by the European Commission

## Slide of the Seminar

# The Dynamics of Finite-sized Particles in Turbulent

***Dr. Samriddhi Sankar Ray***

*ERC Advanced Grant (N. 339032) “NewTURB”  
(P.I. Prof. Luca Biferale)*

Università degli Studi di Roma Tor Vergata  
C.F. n. 80213750583 – Partita IVA n. 02133971008 - Via della Ricerca Scientifica, 1 – 00133 ROMA

# Settling, Collisions, and Coalescences: Droplets in a Turbulent Flow

**Samriddhi Sankar Ray**

**International Centre for Theoretical Sciences  
Tata Institute of Fundamental Research  
Bangalore, India**

15<sup>th</sup> May, 2015

[ssray@icts.res.in](mailto:ssray@icts.res.in)

Department of Physics, University of Rome “Tor Vergata”, Rome

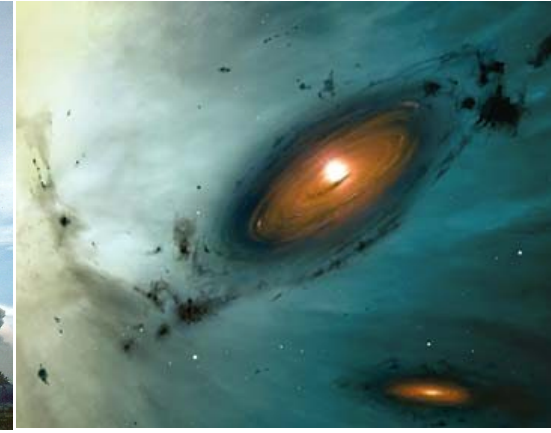
# Why are we interested in particles?



**Cloud formation**



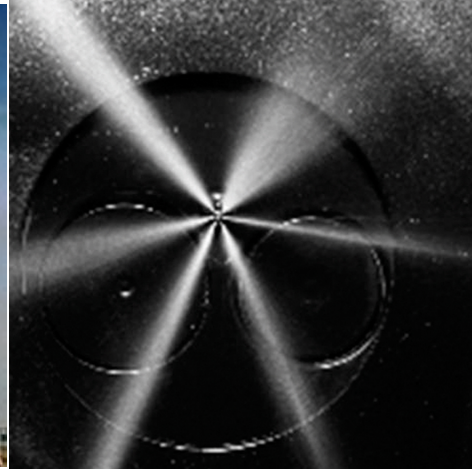
**Pyroclastic flows**



**Planetary formation**



**Pollutant dispersion**



**Industry**



**Planktons and marine biology**

- Finite-sized, Inertial Particles: An Introduction
  - Preferential Concentration
  - Stokes Drag Model
- How Fast do Droplets Collide?
  - Validating the Stokes Drag Model
  - Extreme Events in Relative Velocities
  - Conclusions
- How Fast do Droplets Settle?
  - Settling Velocity
  - Two-particle, Small-scale Properties
    - Correlation Dimension
    - Approaching Rates
  - Conclusions
- Open Questions

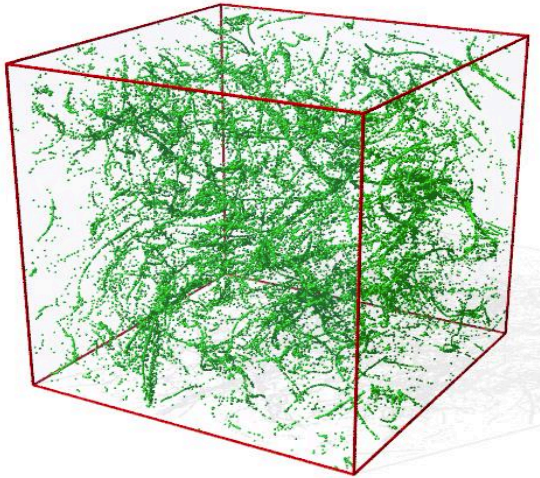


# Inertial Particles

- Density different from that of the fluid.
- Finite size.
- Friction (Stokes) and other forces should be included.
- Velocity different from the underlying fluid velocity.
- Inertial particles have dissipative dynamics: Uniform contraction in phase space.

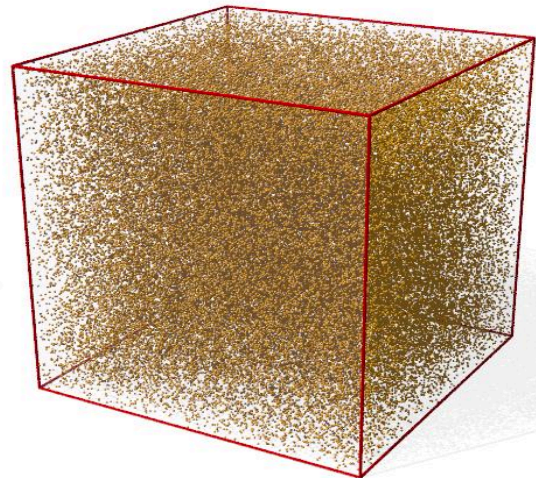
# Types of Particles

$$\beta = \frac{3\rho_f}{\rho_f + 2\rho_p}$$



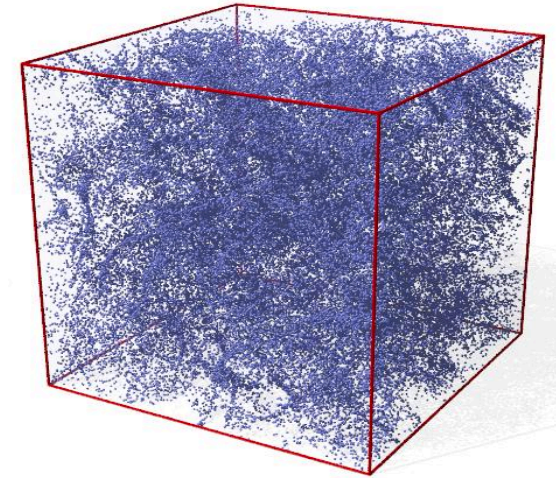
## Light particles

$$\rho_p \ll \rho_f$$
$$\beta = 3$$



## Tracers

$$\rho_p = \rho_f$$
$$\beta = 1$$



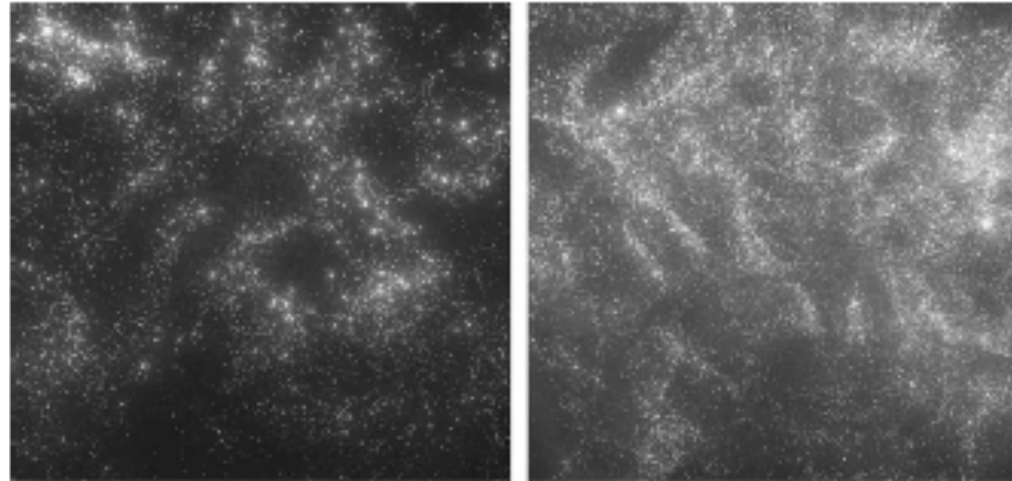
## Heavy particles

$$\rho_p \gg \rho_f$$
$$\beta \ll 1$$

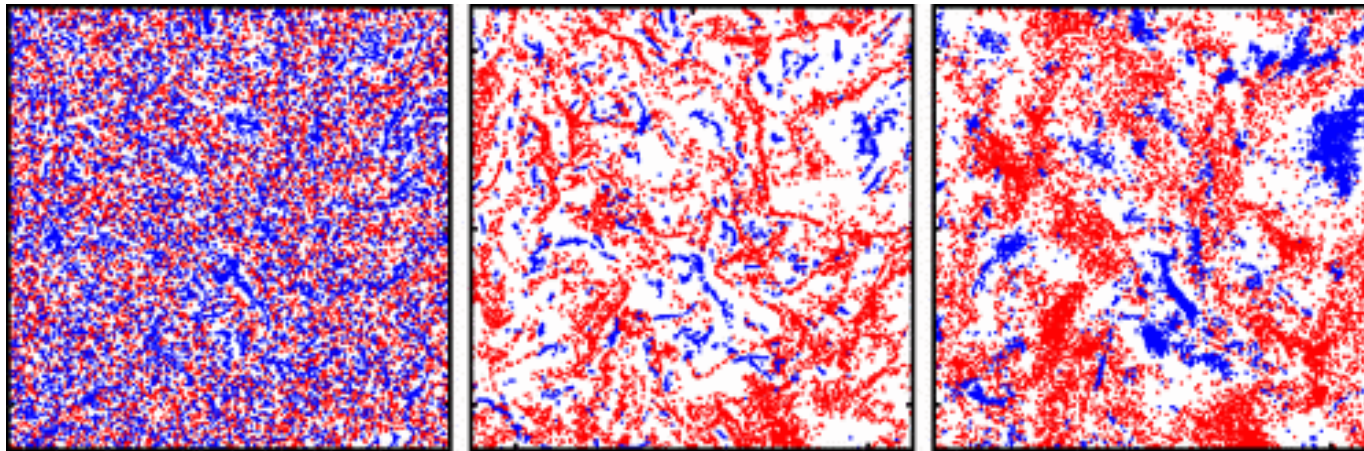
$$\tau_p = \frac{2a^2\rho_p}{9\nu\rho_f}$$

# Effect of Inertia: Preferential Concentration

Experiments:



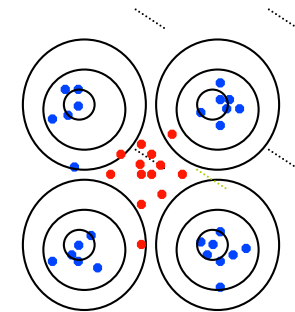
Simulations:



A. M. Wood, *et al.*, *Int. J. Multiphase Flow*, **31** (2005).  
E. Calzavarini, *et al.*, *Phys. Rev. Lett.*, **101** (2008).

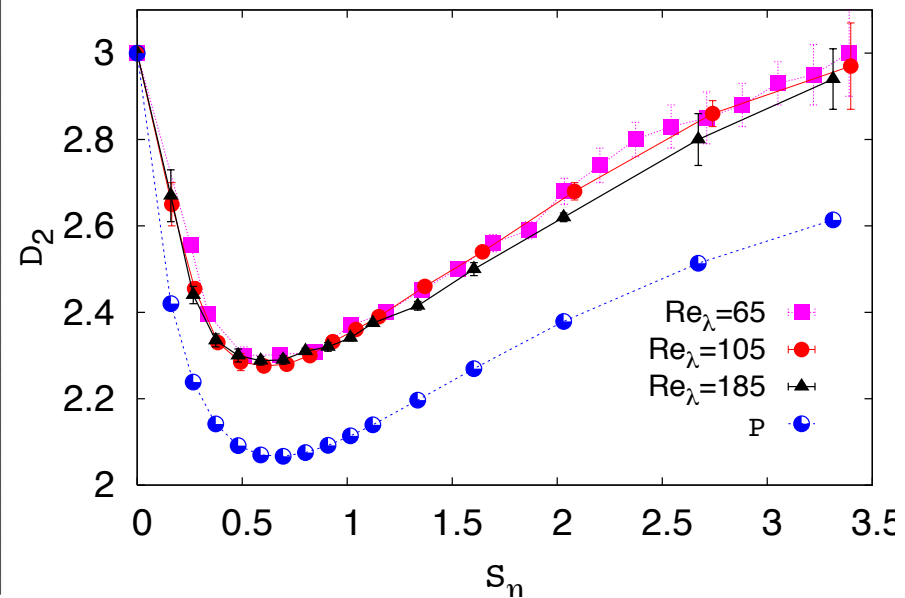
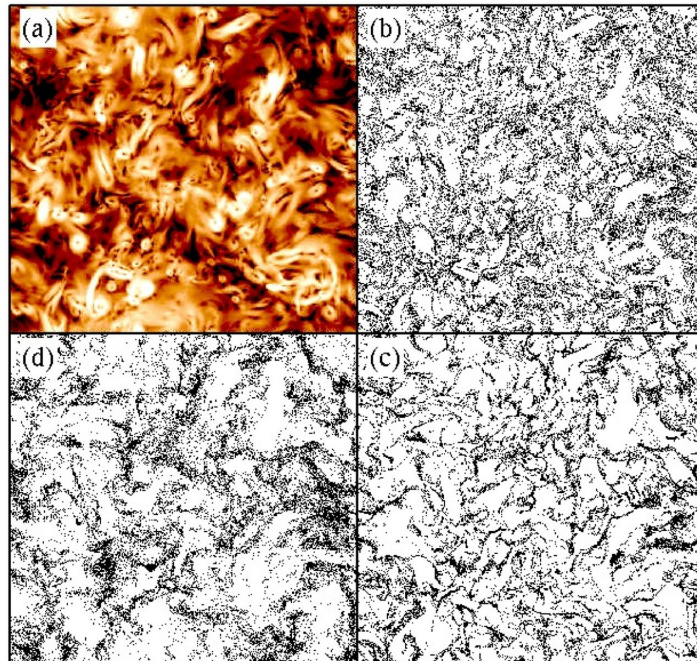
# Understanding Preferential Concentration

- Spatial distribution of finite-size massive particles is strongly inhomogeneous (**preferential concentration**) due to inertia.
- Qualitative understanding based on the idea that vortices act as centrifuges ejecting particles heavier than the fluid and trapping lighter ones.
- $\tau_p \rightarrow 0$  : *uniform distribution*
  - $\dot{\mathbf{x}}_i = \mathbf{u}(\mathbf{x}_i, t)$ ;  $\nabla \cdot \mathbf{u} = 0$ ; assumption of chaoticity.
- $\tau_p \rightarrow \infty$  : *uniform distribution*
  - $\tau_f \ll \tau_p$ ; ballistic motion.
- Maximum clusterization is achieved for a finite value of  $\tau_p$ .
- Small scale particle clusters are characterised by the correlation dimension  $\mathcal{D}_2$  : the probability to find two particles at a distance less than a given  $r$  is  $P_2^<(r) \sim r^{\mathcal{D}_2}$ .





# Preferential Concentration: $\mathcal{D}_2$



(Left) The modulus of the pressure gradient, giving the main contribution to fluid acceleration (a). Particle positions in the same slice are shown for (b)  $St_\eta = 0.16$ , (c)  $0.80$  and (d)  $3.30$ .  
(Right) The correlation dimension  $\mathcal{D}_2$  vs  $St_\eta$  for different  $Re_\lambda$ .

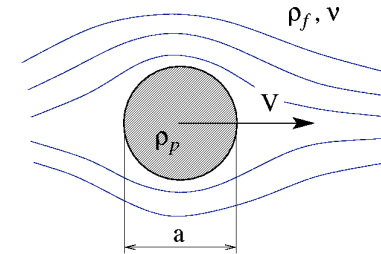
J. Bec, *et al.*, Phys. Rev. Lett. **98** (2007).

J. Bec, *et al.*, Phys. Rev. E **87** (2013).

# Single particle dynamics

Single, passive, spherical, inertial, particle of radius  $a$ , mass  $m_p$ .

$$\begin{aligned}
 \rho_p \frac{d\mathbf{v}}{dt} = & \rho_f \frac{D\mathbf{u}}{Dt} + (\rho_p - \rho_f)\mathbf{g} \\
 & - \frac{9\nu\rho_f}{2a^2} \left( \mathbf{v} - \mathbf{u} - \frac{a^2}{6} \nabla^2 \mathbf{u} \right) \\
 & - \frac{\rho_f}{2} \left( \frac{d\mathbf{v}}{dt} - \frac{D}{Dt} \left[ \mathbf{u} + \frac{a^2}{10} \nabla^2 \mathbf{u} \right] \right)
 \end{aligned}$$



$$\frac{a(u-V)}{\nu} \ll 1 \quad a \ll \eta$$

$\rho_f \frac{D\mathbf{u}}{Dt}$ $\rightarrow$ force by the undisturbed flow; $(\rho_p - \rho_f)\mathbf{g}$ $\rightarrow$ buoyancy;	$\frac{9\nu\rho_f}{2a^2} \left( \mathbf{v} - \mathbf{u} - \frac{a^2}{6} \nabla^2 \mathbf{u} \right)$ $\rightarrow$ Stokes drag; $\frac{\rho_f}{2} \left( \frac{d\mathbf{v}}{dt} - \frac{D}{Dt} \left[ \mathbf{u} + \frac{a^2}{10} \nabla^2 \mathbf{u} \right] \right)$ $\rightarrow$ added mass
---	--

$$D\mathbf{u}/Dt = \partial\mathbf{u}/\partial t + (\mathbf{u} \cdot \nabla)\mathbf{u}$$

$$d\mathbf{u}/dt = \partial\mathbf{u}/\partial t + (\mathbf{v} \cdot \nabla)\mathbf{u}$$



# Stokes Drag Model

## Setting:

- small sized particles;
- dilute suspensions;
- passive particles.

## Simplifications:

- The Faxen correction  $a^2 \nabla^2 \mathbf{u} \approx \mathcal{O}(a^2 u/L) \ll 1$ .
- $\frac{D\mathbf{u}}{Dt} \approx \frac{d\mathbf{v}}{dt}$
- Buoyancy effects negligible.

## Working Equations:

$$\begin{aligned}\frac{d\mathbf{x}}{dt} &= \mathbf{v}; \\ \frac{d\mathbf{v}}{dt} &= -\frac{\mathbf{v} - \mathbf{u}}{\tau_p} + \beta \frac{D\mathbf{u}}{Dt}.\end{aligned}$$

# Stokes Drag Model

## Setting:

- small sized particles;
- dilute suspensions;
- passive particles.

## Simplifications:

- The Faxen correction  $a^2 \nabla^2 \mathbf{u} \approx \mathcal{O}(a^2 u/L) \ll 1$ .
- $\frac{D\mathbf{u}}{Dt} \approx \frac{d\mathbf{v}}{dt}$
- Buoyancy effects negligible.

## Working Equations (for heavy particles):

$$\begin{aligned}\frac{d\mathbf{x}}{dt} &= \mathbf{v}; \\ \frac{d\mathbf{v}}{dt} &= -\frac{\mathbf{v} - \mathbf{u}}{\tau_p}.\end{aligned}$$

- **The Fluid**

- The fluid velocity  $\mathbf{u}$  is a solution of the incompressible Navier–Stokes equation and obtained via pseudo-spectral, direct numerical simulations.
- Statistically steady, homogeneous, isotropic turbulence is maintained by a large-scale forcing.

- **The Particles**

- Particles are much smaller than the Kolmogorov scale, much heavier than the surrounding fluid, and with a small Reynolds number associated to their slip velocity.
- Non-dimensionless numbers:
  - *Stokes number*:  $St = \tau_p / \tau_\eta$ , where  $\tau_\eta = \sqrt{\nu / \varepsilon}$ .
  - *Froude number*:  $Fr = a_\eta / g$ , where  $a_\eta = \varepsilon^{3/4} / \nu^{1/4}$ .

# The Model: Equations

- **The Fluid**

- The incompressible, forced Navier–Stokes equation:

$$\begin{aligned}\partial_t \mathbf{u} + (\mathbf{u} \cdot \nabla) \mathbf{u} &= -\nabla p + \nu \nabla^2 \mathbf{u} + \mathbf{f}; \\ \nabla \cdot \mathbf{u} &= 0.\end{aligned}$$

- $\nu$  is the fluid kinematic viscosity and  $\mathbf{f}$  a large scale forcing.

- **The Particles**

- Stokes drag and gravity:

$$\begin{aligned}\frac{d\mathbf{x}_p}{dt} &= \mathbf{v}_p; \\ \frac{d\mathbf{v}_p}{dt} &= -\frac{1}{\tau_p} [\mathbf{v}_p - \mathbf{u}(\mathbf{x}_p, t)] + \mathbf{g}.\end{aligned}$$

- $\mathbf{u}(\mathbf{x}_p, t)$  is evaluated by linear interpolation.

# How Fast do Droplets Collide?

## Extreme fluctuations of the relative velocities between droplets in turbulent airflow

- Experiments (*with* Ewe-Wei Saw, Gregory P. Bewley, and Eberhard Bodenschatz, Göttingen, Germany)
- Theory and Direct Numerical Simulations (*with* Jérémie Bec, Nice, France)

Ewe-Wei Saw, Gregory P. Bewley, Eberhard Bodenschatz, Samriddhi Sankar Ray, and Jérémie Bec  
*Physics of Fluids Letters*, 26, 111702 (2014).

- In warm clouds, turbulence in the airflow enhances the collision rate of the water droplets.
- It thus influences the evolution of droplet sizes and the timescale for rain formation.
- Two mechanisms are at play:
  - preferential concentration;
  - very large approach velocities explained in terms of the *sling effect* and the subsequent formation of *caustics*.
- Open question regarding the coalescence rate of droplets.
  - Collisions that are too violent can cause particle fragmentation.
- Developing an understanding:
  - Experiments
  - Theory
  - Direct Numerical Simulations

G. Falkovich, *et al*, Nature **419**, (2002).  
R. Shaw, Ann. Rev. Fluid Mech. **35** (2003).  
E.-W. Saw, *et al.*, Phys. Rev. Lett. **100** (2008).  
M. Wilkinson, *et al*, Phys. Rev. Lett. **97** (2006).

E. Balkovsky, *et al.*, Phys. Rev. Lett. **86** (2001).  
J. Bec, *et al*, Phys. Rev. Lett. **98** (2007).  
G. P. Bewley, *et al.*, New J. Phys. **15** (2013).  
G. Falkovich & A. Pumir, J. Atmos. Sci. **64** (2007).



**What is the distribution of relative velocities of colliding droplets in a turbulent airflow?**

**Is the linear Stokes drag model valid?**

We perform direct numerical simulations and experiments, with matching parameters, of droplets in a turbulent flow to answer these two questions.

# Experiment

- Homogeneous and isotropic turbulent flows are generated in a 1 *m*-diameter acrylic sphere by 32 randomly pulsating jets in a region of about 10 *cm* at the center.
- We ran the experiment for  $R_\lambda = 160$  ( $\eta = 300\mu m$ ), 170 ( $\eta = 230\mu m$ ), and 190 ( $\eta = 180\mu m$ ).
- Droplets are produced with a spinning disc device that eject bi-disperse drops with diameters  $6.8\mu m$  and  $19\mu m$ .
- The motion of the droplets are measured by an imaging of their shadows projected by white light sources.
- The three-dimensional positions of the droplets are determined by stereoscopic Lagrangian Particle Tracking.

G. P. Bewley, *et al.*, *New J. Phys.* **15** (2013).

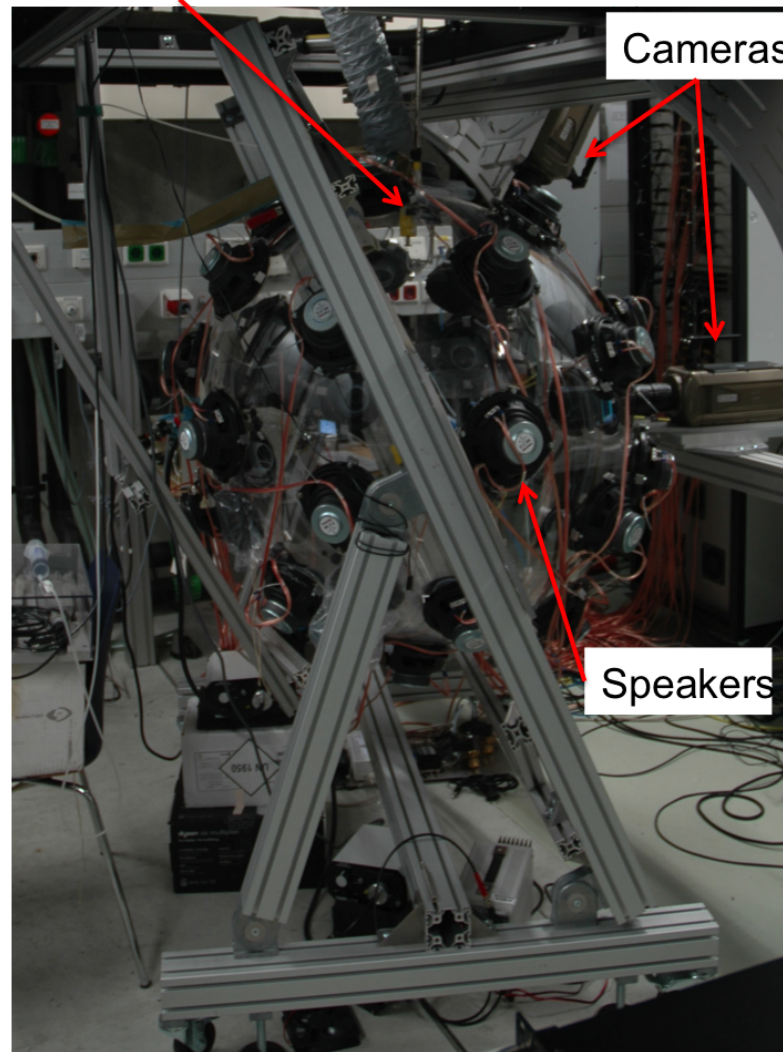
W. H. Walton & W. C. Prewett, *Proc. Phys. Soc. B* **62** (1949).

K. Chang, *et al.*, *J. Fluid Mech.* **692** (2012).

N. Ouellette, *et al.*, *New J. Phys.* **8** (2006).

# Experiment: Soccer Ball

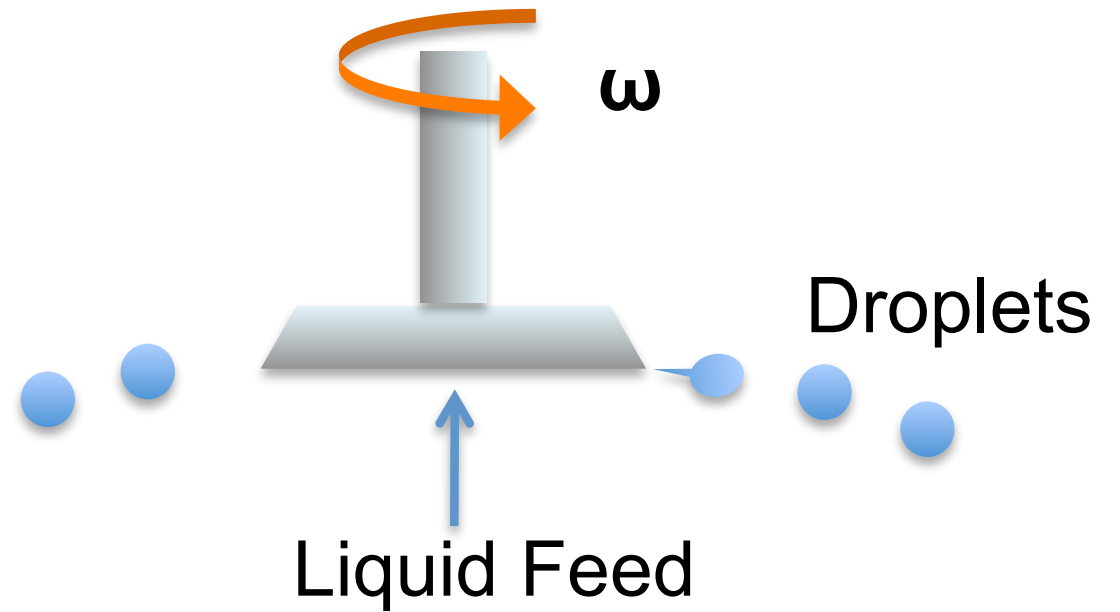
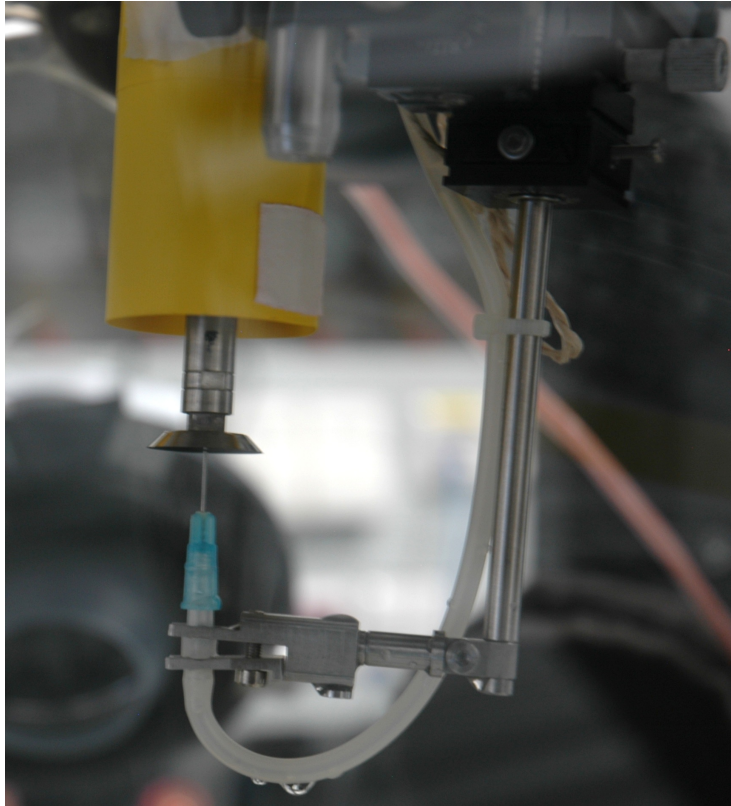
Droplet generator



Cameras

Speakers

# Experiment: Droplet Generator



# Direct Numerical Simulations (DNS)

- **The Fluid**

- The incompressible, forced Navier–Stokes equation:

$$\begin{aligned}\frac{\partial \mathbf{u}}{\partial t} + (\mathbf{u} \cdot \nabla) \mathbf{u} &= -\nabla p + \nu \nabla^2 \mathbf{u} + \mathbf{f}; \\ \nabla \cdot \mathbf{u} &= 0.\end{aligned}$$

- Pseudo-spectral parallel solver for the fluid velocity with  $512^3$  grid points and  $\nu = 1.5 \times 10^{-4}$  ( $R_\lambda = 180$ ).

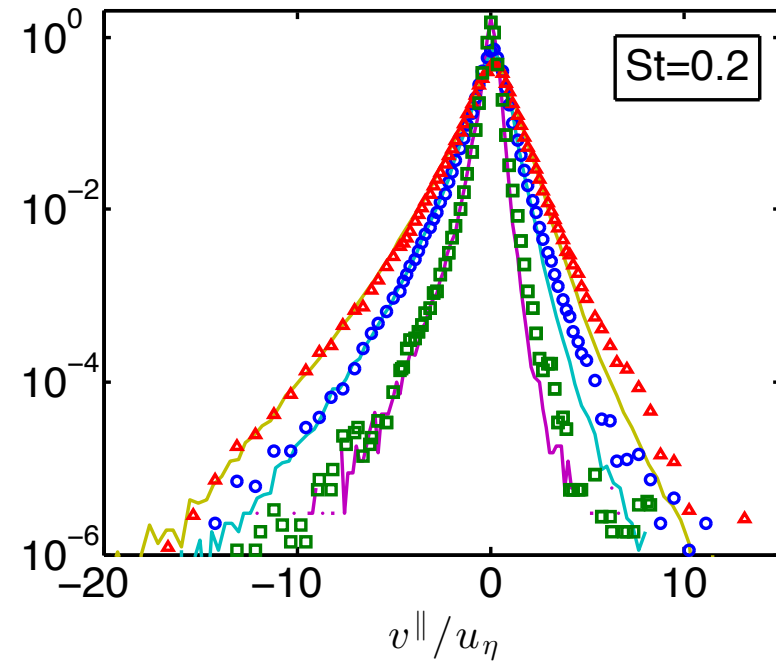
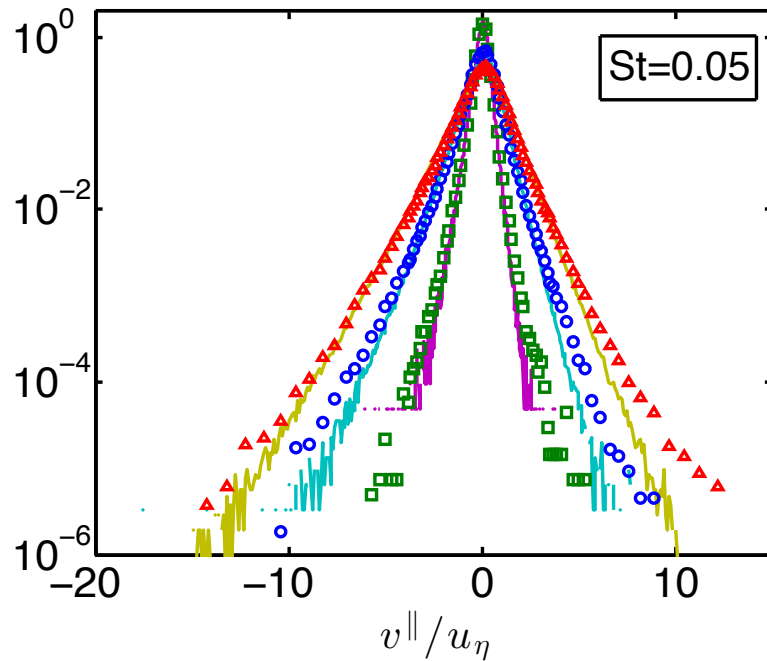
- **The Particles**

- Stokes drag and gravity:

$$\begin{aligned}\frac{d\mathbf{x}_p}{dt} &= \mathbf{v}_p; \\ \frac{d\mathbf{v}_p}{dt} &= -\frac{1}{\tau_p} [\mathbf{v}_p - \mathbf{u}(\mathbf{x}_p, t)] + \mathbf{g}.\end{aligned}$$

- $\mathbf{u}(\mathbf{x}_p, t)$  is evaluated by linear interpolation.
- Number of particles  $N_p = 10^8$ .

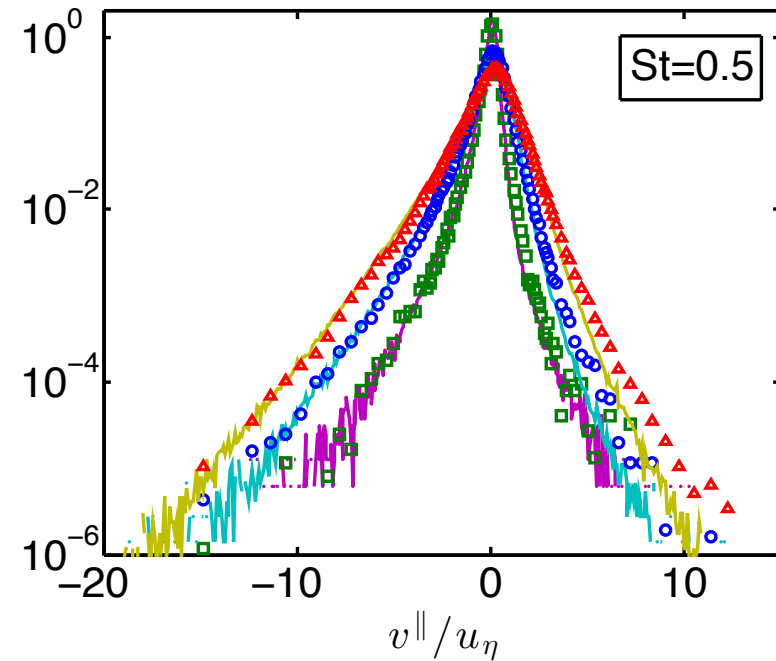
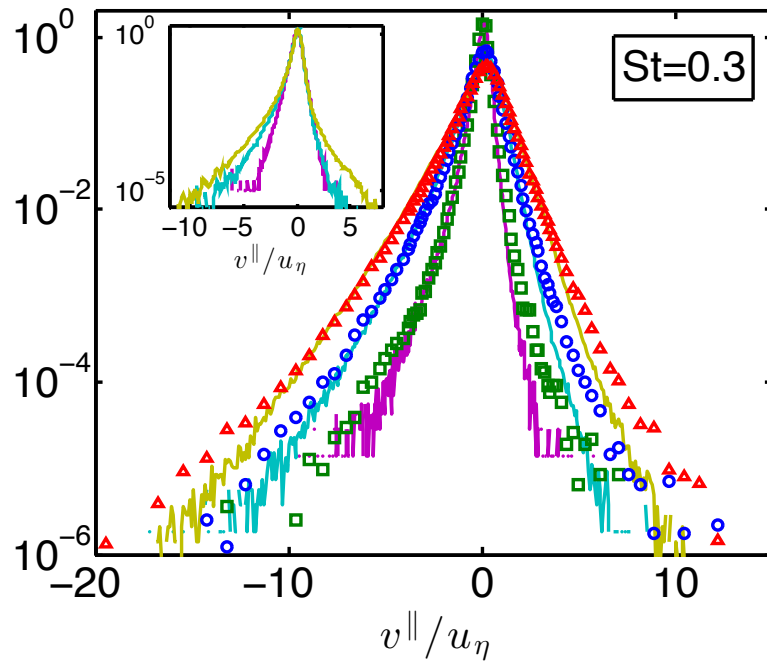
# Relative Velocity: PDF



Probability distribution functions of the longitudinal velocity differences conditioned on different separations  $r$  for particles with (left)  $St = 0.05$  ( $St_{DNS} = 0.05$ ,  $St_{\text{experiment}} = 0.04$ ) and (right)  $St = 0.2$  ( $St_{DNS} = 0.24$ ,  $St_{\text{experiment}} = 0.19$ ). The symbols are the experimental data and solid lines are the DNS data. In all panels, for the experiment (DNS) data, squares (purple) correspond to  $r = 1 - 1.6\eta$ , circles (cyan) to  $r = 3 - 3.6\eta$ , and triangles (gold) to  $r = 5 - 5.6\eta$ .



# Relative Velocity: PDF



Probability distribution functions of the longitudinal velocity differences conditioned on different separations  $r$  for particles with (left)  $St = 0.3$  and (right)  $St = 0.5$ . The symbols are the experimental data and solid lines are the DNS data. In all panels, for the experiment (DNS) data, squares (purple) correspond to  $r = 1 - 1.6\eta$ , circles (cyan) to  $r = 3 - 3.6\eta$ , and triangles (gold) to  $r = 5 - 5.6\eta$ . The inset shows the variation with respect to  $St$ , with the separation fixed to  $r = 1 - 1.6\eta$ . From the bottom to the top curve,  $St = 0.05, 0.3, 0.5$ .

# Validity of the Stokes Drag Model?

- Quantitatively, we found the differences between experiments and simulations to be less than about 15% in the core of the distributions.
- Similarly, we found excellent agreement in the tails of the distributions, but only for the largest Stokes number ( $St = 0.5$ ), the smallest scale ( $r < 2\eta$ ), and for the left side of the distributions corresponding to approaching particle pairs.
- In other cases, the experimental tails of the PDFs increasingly deviate from the simulated ones as one moves to higher relative velocities.
- The discrepancy is larger in the right tails, corresponding to separating pairs, where in the worst case the experimental data is about 5 times above the simulated data.
- In the left tails, the discrepancy is less severe, but worsens with decreasing  $St$ , so that the largest discrepancy is a factor of two.

# Possible Causes of Discrepancy

- Effects beyond linear Stokes drag maybe at play.
  - The history term may play an important role, which, given the experimental conditions, is the first subdominant correction.
- Measurement uncertainty.
  - We characterized the measurement noise and add it to the DNS data.
  - Estimated  $\varepsilon$ , in the experiment by applying the same method to the DNS data to obtain a 5% agreement.
  - We ruled out the possibility of a Reynolds number effect by comparing DNS data at increasing Reynolds numbers.
  - Inaccuracy of  $\nu$  in the experiment was checked by reprocessing the experimental data with a modified  $\nu$  ( $\pm 30\%$ ) with no clear improvement.
- No clear explanation for the discrepancies.
- The influences of nonlinear forces, hydrodynamic interactions, and non-universal turbulence statistics merit further study.

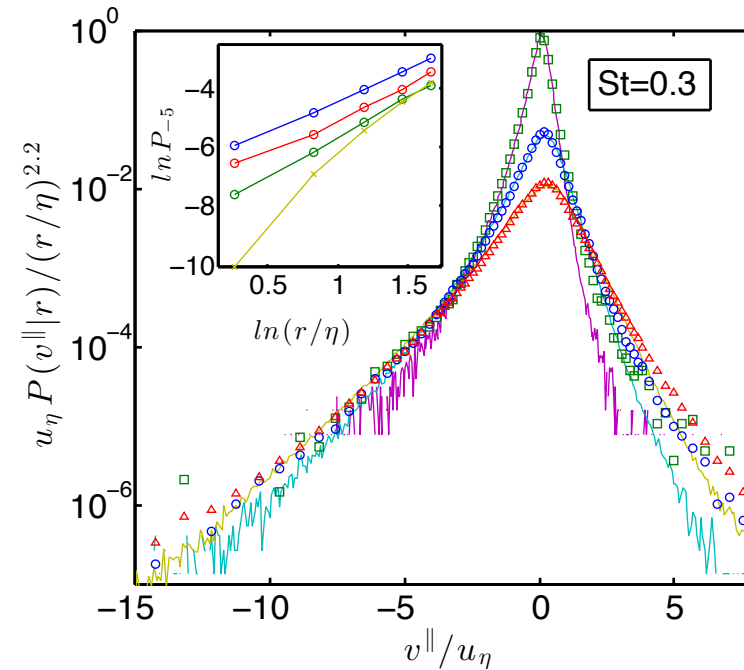
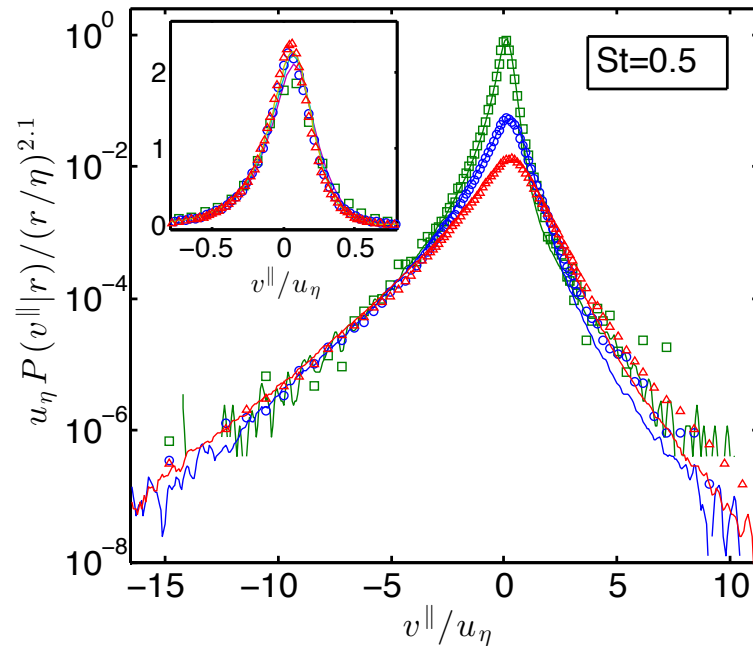
# Velocities of Colliding Droplets

- There is general agreement in the trends and shapes of the distributions.
- All the distributions can be approximated by stretched-exponentials whose concavity increases with increasing  $St$  and decreasing  $r$ .
- This is qualitatively consistent with what is known about the velocity distributions of fluid particles.
- Earlier prediction of *compressed* exponential distributions for very large  $St$  not observed.
  - The distributions we measure are stretched rather than compressed, and the implication is that the large  $St$  limit taken in the theory does not accurately describe the intermediate  $St$  dynamics studied here.

# Scale-dependence of Relative Velocities

- To understand droplet collision-coalescence in clouds, one needs to characterize droplet relative velocities at contact.
- Hence it is important to understand how droplet relative velocities scale with vanishing  $r$ .
- Experimental and DNS data collapse at large negative values of  $v^{\parallel}$  when the PDF is rescaled by  $r^{\beta}$  with  $\beta \approx 2.1$ .
- Such collapse indicates that the distribution of approaching velocities takes the form  $p(v^{\parallel} | r) \simeq r^{\beta}(St) \phi(v^{\parallel})$  at sufficiently small separations and large velocities.
- This behavior is expected to extend down to separations of the order of the particle size and hence should describe the distribution of violent impact velocities between particles.

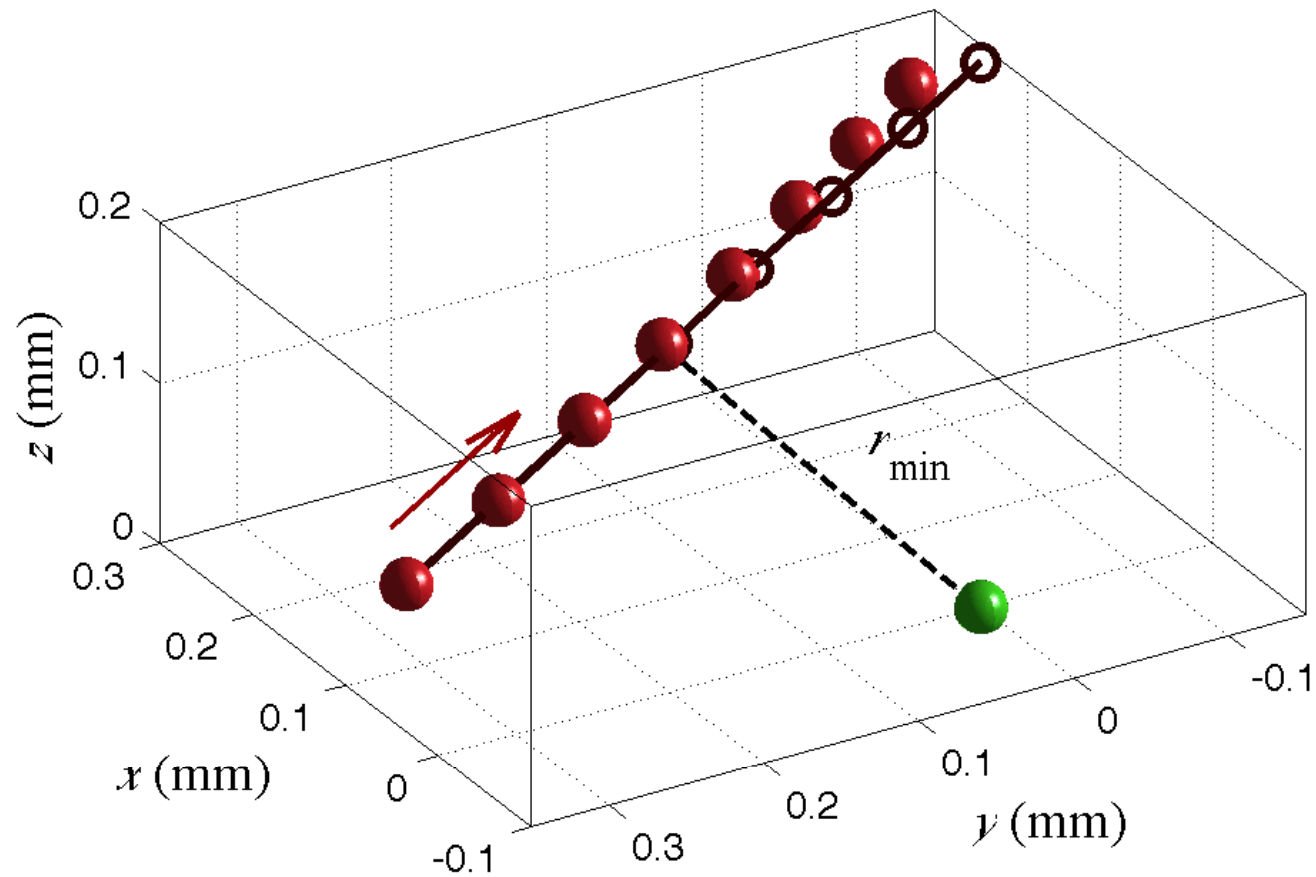
# Relative Velocity: Rescaled PDF



Rescaled probability distributions of the longitudinal velocity difference conditioned on different separations  $r$  for both the experimental (symbols) and DNS (solid lines) data for (left)  $St = 0.5$  with  $\beta = 2.1$  and (right)  $St = 0.3$ , with  $\beta = 2.2$ . Green corresponds to  $r = 1 - 1.6\eta$ , blue to  $r = 3 - 3.6\eta$ , and red to  $r = 5 - 5.6\eta$ . Inset (left):  $r$ -scaling of the distribution bulk; collapse is attained by  $r \times p(v^{\parallel}|r)$  and  $(1/r) \times v^{\parallel}/u_{\eta}$ . Inset (right): plots of  $\ln[\text{Pr}(v^{\parallel}/u_{\eta} < 5 | r)]$  (denoted as  $\ln P_{-5}$ ) versus  $\ln(r/\eta)$  for different  $St$  from the experiment. Unambiguous values of  $\beta$  could not be obtained at such low  $St$ .



# Reconstructing Particle Tracks



Reconstructing tracks of individual particles.

# Conclusions

- We evaluated the accuracy of the Stokes drag model by comparing results from DNS with experimental measurements.
- For relative velocities, the DNS matched all qualitative trends of the experiments.
- Quantitative agreements for inertia-dominated regimes.
- Discrepancies found in some regimes.
- No trivial explanations for such discrepancies.
  - Corrections to the Stokes drag model.
  - Hydrodynamic interactions between particles.
  - Small-scale, non-universality of the turbulence.
- For inertial particles, at dissipative scales of turbulence:

$$p(v^{\parallel} | r) \simeq r^{\beta(St)} \phi(v^{\parallel}).$$

# How Fast do Droplets Settle Under Gravity?

## Gravity-driven enhancement of heavy particle clustering in turbulent flow

- Direct Numerical Simulations
- Theory: Asymptotic Expansion

**J r mie Bec, Holger Homann, and Samriddhi Sankar Ray.**  
**Physical Review Letters 112, 184501 (2014)**

- Many industrial, atmospheric, and astrophysical phenomena involves the interactions between small solid particles suspended in a turbulent carrier flow.
- Two main effects:
  - a viscous drag on the particles (*dominant for small particles*);
  - external forces, such as gravity, on the particles (*dominant for large particles*).
- Standard modelling treats these two limits separately and often fails at the interface.
  - Example: the rate at which rain is triggered in warm clouds.
- An improvement might be to combine the effects of turbulence and gravity.

G. Falkovich, *et al*, Nature **419**, (2002).

W. Grabowski & L.-P. Wang, *Annu. Rev. Fluid Mech.* **45**, (2013).

- In turbulent flows, there is an increase of the terminal velocity of heavy particles.
- This phenomenon is mostly understood on qualitative grounds and has been quantified only in model flows.
- Very little is known on the effect of gravitational settling on two-particle statistics.
- Fundamental theoretical and numerical studies of the clustering of particle pairs and of the enhancement of collisions due to inertia usually neglect gravity.

M. Maxey, *J. Fluid Mech.* **174**, (1987).

L.-P. Wang & M. Maxey, *J. Fluid Mech.* **256**, 27 (1993).

E. Balkovsky, *et al*, *Phys. Rev. Lett.* **86**, (2001).

J. Davila & J. Hunt, *J. Fluid Mech.* **440**, (2001).

M. Wilkinson, *et al*, *Phys. Rev. Lett.* **97**, (2006).

O. Ayala, *et al*, *New J. Phys.* **10**, (2008).

J. Bec, *et al*, *Phys. Rev. Lett.* **98**, (2007).

J. Bec, *et al*, *Fluid Mech.* **646**, (2010).

## **What is the interplay between turbulence, gravity, and particle sizes?**

Important for fluid dynamics and non-equilibrium statistical physics.

# Our Approach

- We combine direct numerical simulations with theoretical results based on *standard* asymptotic analysis.
- We make a systematic study of the dynamical and statistical properties of particles as a function of
  - the level of turbulence of the carrier flow (Reynolds number);
  - the inertia of the particles (Stokes number);
  - the ratio between the turbulent accelerations and gravity (Froude number).



- **The Fluid**

- The fluid velocity  $\mathbf{u}$  is a solution of the incompressible Navier–Stokes equation and obtained via pseudo-spectral, direct numerical simulations.
- Statistically steady, homogeneous, isotropic turbulence is maintained by a large-scale forcing.

- **The Particles**

- Particles are much smaller than the Kolmogorov scale, much heavier than the surrounding fluid, and with a small Reynolds number associated to their slip velocity.
- Non-dimensionless numbers:
  - *Stokes number*:  $St = \tau_p / \tau_\eta$ , where  $\tau_\eta = \sqrt{\nu / \varepsilon}$ .
  - *Froude number*:  $Fr = a_\eta / g$ , where  $a_\eta = \varepsilon^{3/4} / \nu^{1/4}$ .
- We use 10 different Stokes numbers and 5 different values of the Froude number

# The Model: Equations

- **The Fluid**

- The incompressible, forced Navier–Stokes equation:

$$\begin{aligned}\partial_t \mathbf{u} + (\mathbf{u} \cdot \nabla) \mathbf{u} &= -\nabla p + \nu \nabla^2 \mathbf{u} + \mathbf{f}; \\ \nabla \cdot \mathbf{u} &= 0.\end{aligned}$$

- $\nu$  is the fluid kinematic viscosity and  $\mathbf{f}$  a large scale forcing.

- **The Particles**

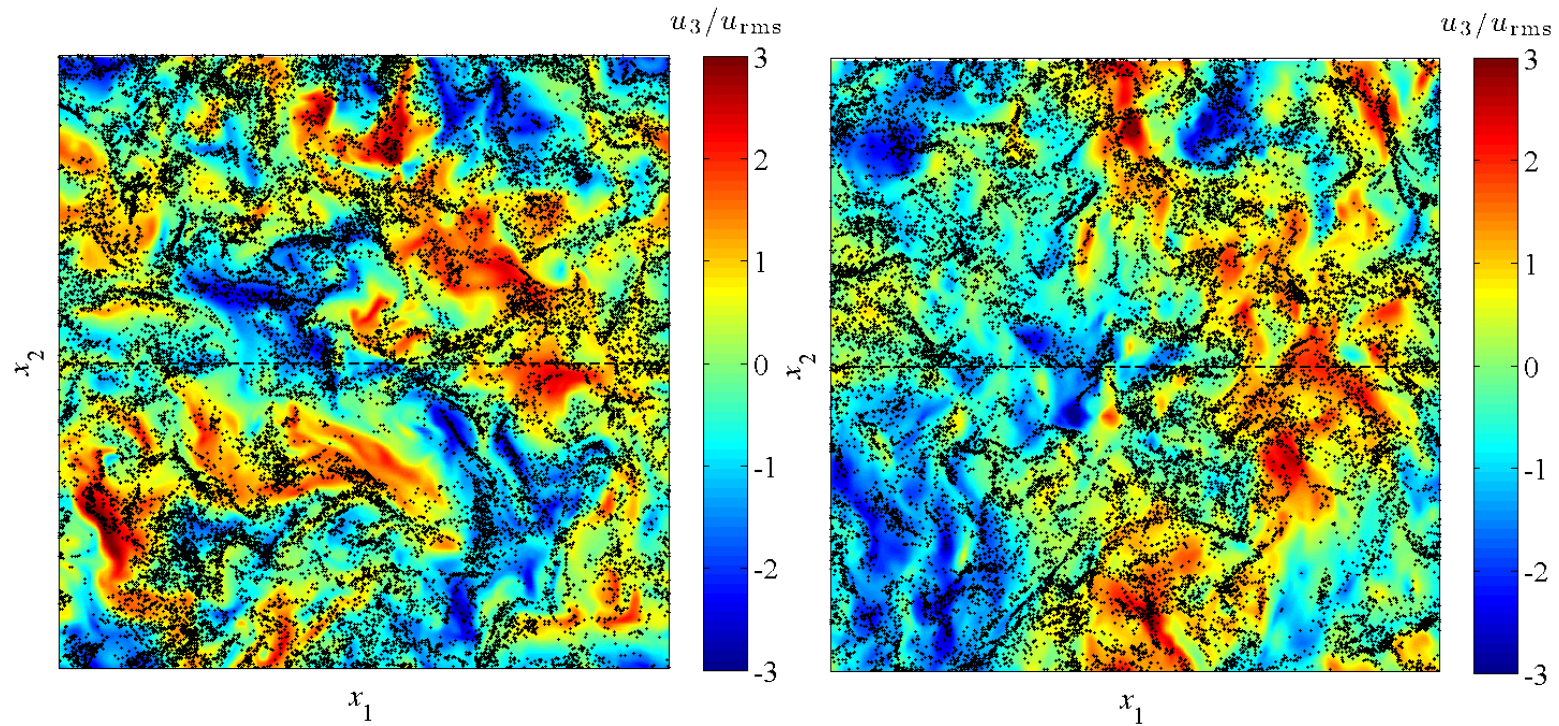
- Stokes drag and gravity:

$$\begin{aligned}\frac{d\mathbf{x}_p}{dt} &= \mathbf{v}_p; \\ \frac{d\mathbf{v}_p}{dt} &= -\frac{1}{\tau_p} [\mathbf{v}_p - \mathbf{u}(\mathbf{x}_p, t)] + \mathbf{g}.\end{aligned}$$

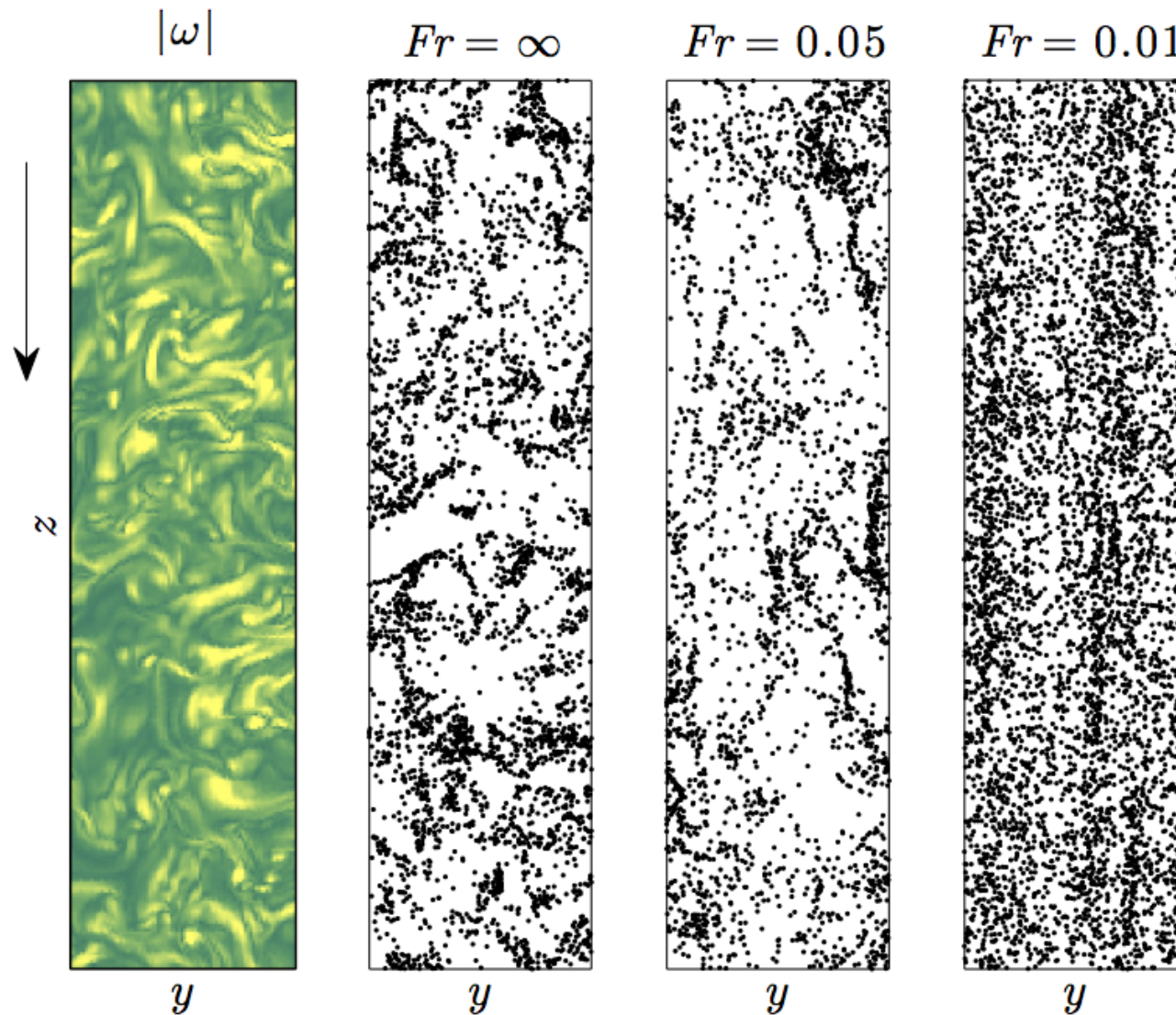
- $\mathbf{u}(\mathbf{x}_p, t)$  is evaluated by linear interpolation.

# Simulation: Details

$Re_\lambda$	$u_{\text{rms}}$	$\Delta t$	$\eta$	$\tau_\eta$	$L$	$T_L$	$N^3$	$N_p$
460	0.189	0.0012	$1.45 \times 10^{-3}$	0.083	1.85	9.9	$2048^3$	$10 \times 10^8$
290	0.185	0.003	$2.81 \times 10^{-3}$	0.131	1.85	9.9	$1024^3$	$1.28 \times 10^8$
127	0.144	0.02	$1.12 \times 10^{-2}$	0.45	2.11	14.6	$256^3$	$0.08 \times 10^8$



# Particle Distribution: Effect of Gravity



Snapshot of the vorticity modulus (Left; yellow = low values, green = high values) and of the particle positions for  $R_\lambda = 130$ ,  $St = 1$  and three different values of the Froude number in a slice of thickness  $10\eta$ , width  $130\eta$ , and height  $520\eta$ . The vertical arrow indicates gravity.

# Settling Velocity: Qualitative Understanding

- Define : The average settling velocity  $V_g = -\langle \mathbf{v}_p \cdot \hat{\mathbf{e}}_z \rangle$ .
- Statistical stationarity  $\implies V_g = \tau_p g - \langle u_z(\mathbf{x}_p, t) \rangle$ .
- Define : The relative increase in settling velocity:

$$\Delta_V = (V_g - \tau_p g) / (\tau_p g) = -\langle u_z(\mathbf{x}_p, t) \rangle / (\tau_p g)$$

- *If* settling particles in a turbulent flow sample regions where the vertical fluid velocity is aligned with gravity, we expect an enhancement of the average settling velocity.

M. Maxey, J. Fluid Mech. **174**, (1987).

L.-P. Wang & M. Maxey, J. Fluid Mech. **256**, 27 (1993).

K. Gustavsson, *et al.*, Phys. Rev. Lett. **112**, 214501 (2014).



# Settling Velocity: Qualitative Understanding



- Define : The average settling velocity  $V_g = -\langle \mathbf{v}_p \cdot \hat{\mathbf{e}}_z \rangle$ .
- Statistical stationarity  $\implies V_g = \tau_p g - \langle u_z(\mathbf{x}_p, t) \rangle$ .
- Define : The relative increase in settling velocity:

$$\Delta_V = (V_g - \tau_p g) / (\tau_p g) = -\langle u_z(\mathbf{x}_p, t) \rangle / (\tau_p g)$$

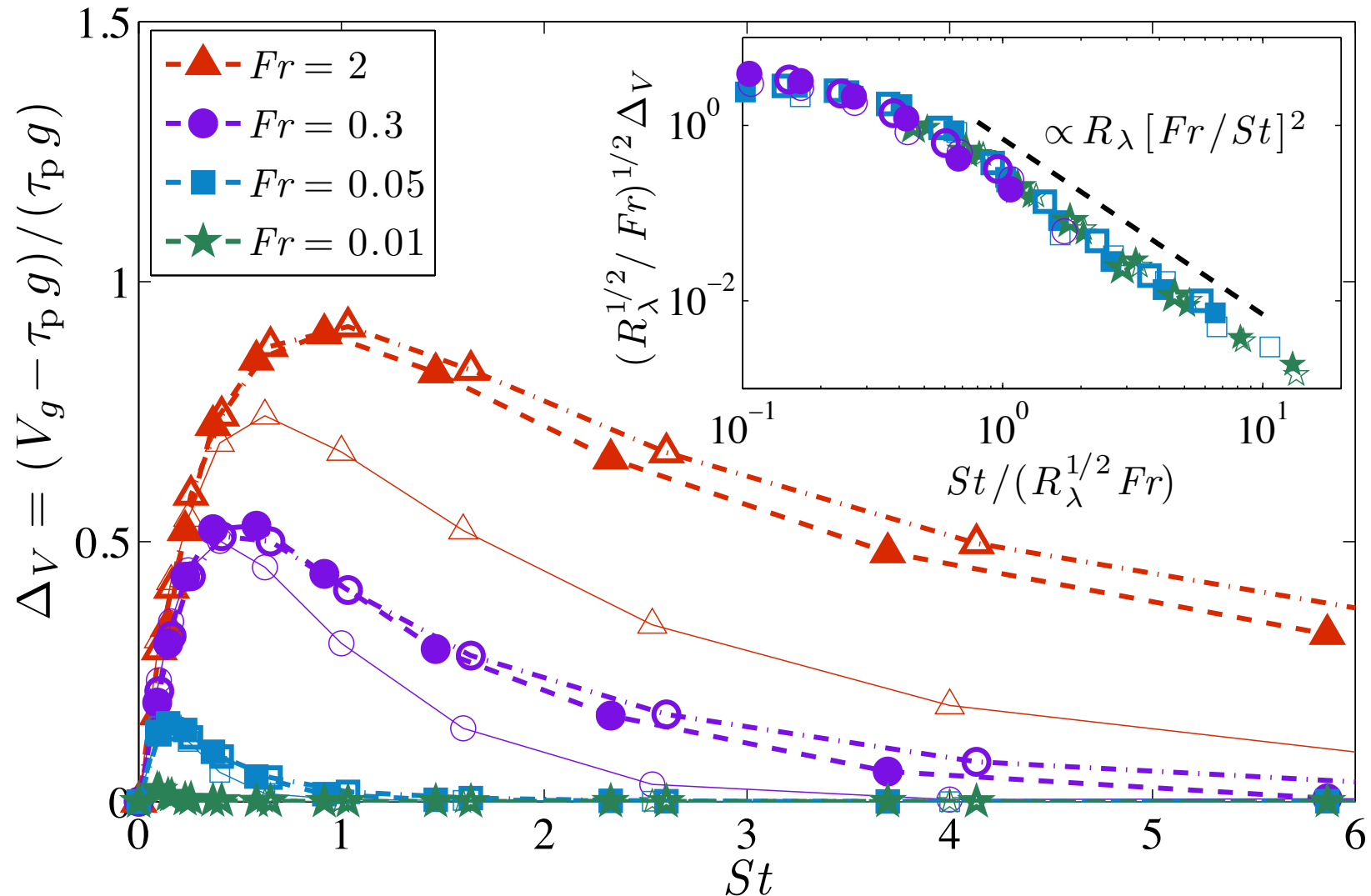
- What is its dependence on the particle Stokes number and for different values of  $Fr$  and  $R_\lambda$ ?
- *If* settling particles in a turbulent flow sample regions where the vertical fluid velocity is aligned with gravity, we expect an enhancement of the average settling velocity.
  - Is there a way to see this preferential sampling from the equations of motion?

M. Maxey, J. Fluid Mech. **174**, (1987).

L.-P. Wang & M. Maxey, J. Fluid Mech. **256**, 27 (1993).

K. Gustavsson, *et al.*, Phys. Rev. Lett. **112**, 214501 (2014).

# Settling Velocity



Relative increase of the settling velocity  $\Delta_V$  as a function of the Stokes number  $St$  for various Froude numbers, as labeled, and  $R_\lambda = 130$  (thin symbols, plain lines),  $R_\lambda = 290$  (filled symbols, dashed lines) and  $R_\lambda = 460$  (open symbols, broken lines). Inset:  $[R_\lambda^{1/2}/Fr]^{1/2}\Delta_V$  as a function of  $St/[R_\lambda^{1/2}Fr]$  for the same data.



## Small Stokes Asymptotics

- **Why is there an enhancement?**

- To leading order, the particles advected by an effective velocity field:

$$\mathbf{v} = \mathbf{u} + \tau_p \mathbf{g} - \tau_p [\partial_t \mathbf{u} + (\mathbf{u} + \tau_p \mathbf{g}) \cdot \nabla \mathbf{u}].$$

- Focus on the  $(x, y)$  plane.
- By using isotropy and incompressibility, we obtain:

$$\langle u_z \nabla_{\perp} \cdot \mathbf{v}_{\perp} \rangle = \tau_p^2 g \langle (\partial_z u_z)^2 \rangle > 0.$$

## Small Stokes Asymptotics

- **Why is there an enhancement?**

- To leading order, the particles advected by an effective compressible velocity field:

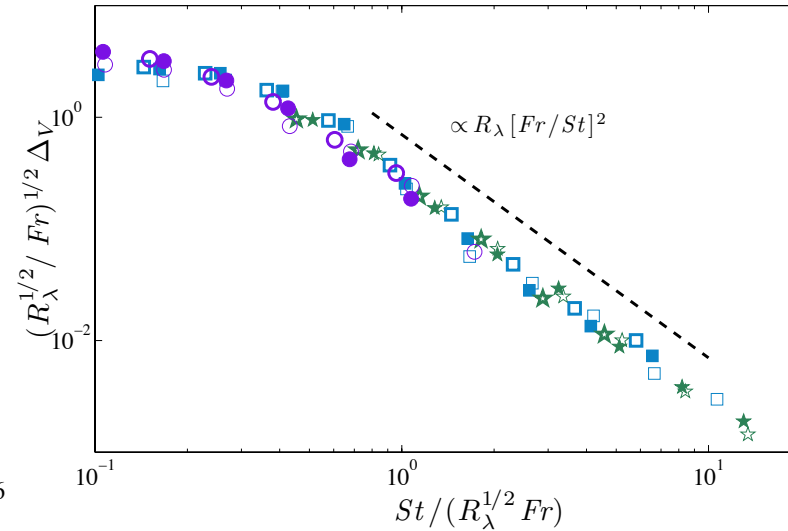
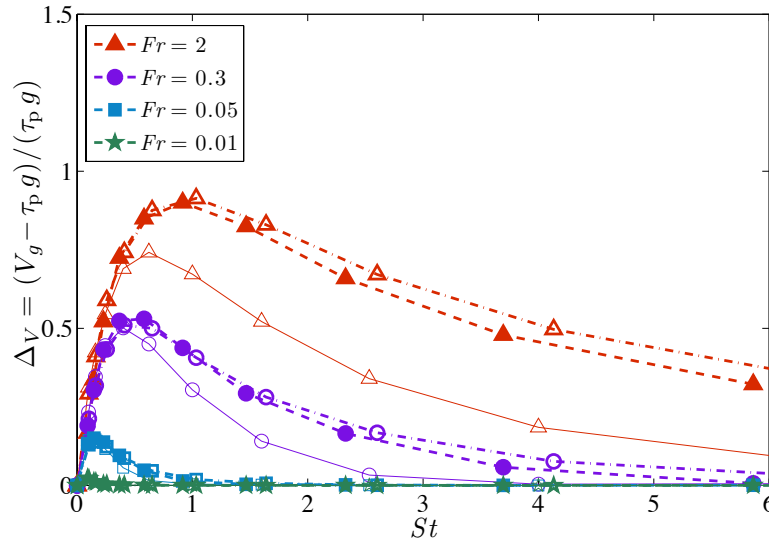
$$\mathbf{v} = \mathbf{u} + \tau_p \mathbf{g} - \tau_p [\partial_t \mathbf{u} + (\mathbf{u} + \tau_p \mathbf{g}) \cdot \nabla \mathbf{u}].$$

- Focus on the  $(x, y)$  plane.
- By using isotropy and incompressibility, we obtain:

$$\langle u_z \nabla_{\perp} \cdot \mathbf{v}_{\perp} \rangle = \tau_p^2 g \langle (\partial_z u_z)^2 \rangle > 0.$$

- *Particles preferentially cluster (negative divergence), on average, in the  $(x, y)$  plane, at points where the fluid velocity is vertically downwards ( $u_z < 0$ ).*

# Settling Velocity: Quantitative Understanding



## Small Stokes Asymptotics

$$\Delta V \propto \tau_\eta \tau_p \langle (\partial_z u_z)^2 \rangle \propto St$$

Assumptions & Algorithm:

- Relate  $V_g$  to  $\langle u_z \nabla_\perp \cdot \mathbf{v}_\perp \rangle$ .
- Hence  $\langle u_z(\mathbf{X}_p, t) \rangle \propto \tau_\eta \langle u_z \nabla_\perp \cdot \mathbf{v}_\perp \rangle$ .

## Large Stokes Asymptotics

$$\Delta V \propto R_\lambda^{3/4} Fr^{5/2} St^{-2}$$

Valid:

- $St \gg R_\lambda^{1/2} Fr$  and  $Fr \ll R_\lambda^{1/2}$ .

# Small-scale, Two-particle Statistics

- Describe the evolution of pair separations in terms of  $\nabla \mathbf{u}$ .
- $V_g \gg u_\eta$ : the particles travel  $\eta$  in a time shorter than  $\tau_\eta$ .
- Rescale time by  $\tau_\eta(V_g/u_\eta)$  and space by  $\eta$ :

$$\frac{d^2 \mathbf{R}}{ds^2} \simeq -\frac{1}{\tilde{S}} \left[ \frac{d\mathbf{R}}{ds} - \mathbf{R} \cdot \boldsymbol{\sigma}(s) \right],$$

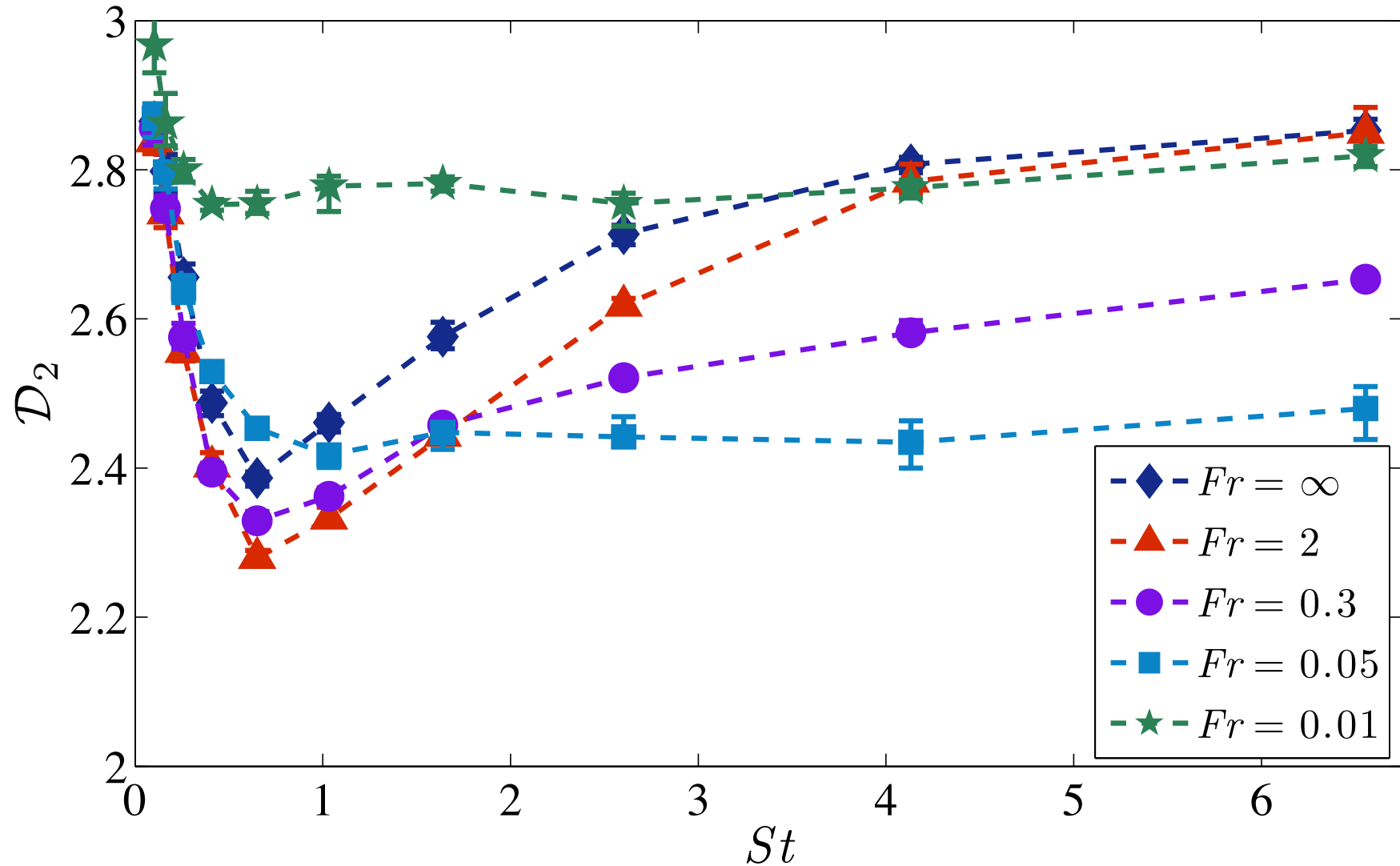
where  $\boldsymbol{\sigma}$  is a Gaussian tensorial noise with co-variance  $\langle \sigma_{ij}(s) \sigma_{kl}(s') \rangle = (\nu/\varepsilon) \langle \partial_i u_j \partial_k u_\ell \rangle \delta(s - s')$ .

- The effective Stokes number  $\tilde{S} = St(u_\eta/V_g)$ .
- $V_g \gg u_\eta$ : small-scale two-particle statistics depend only on  $\tilde{S}$ .
- When  $\Delta_V \ll 1$ ,  $\tilde{S} \simeq Fr$ ; the statistics become independent of  $St$  when  $St \gg Fr$ .

## $\mathcal{D}_2$ : The Correlation Dimension

- An important observable measuring particle clustering is the correlation dimension  $\mathcal{D}_2$  of their spatial distribution.
- It is given by  $\mathbb{P}_2(r) \propto r^{\mathcal{D}_2}$  for  $r \ll \eta$ , where  $\mathbb{P}_2(r)$  is the probability that two particles are within a distance  $r$ .

# $\mathcal{D}_2$ : Correlation Dimension



Correlation dimension  $\mathcal{D}_2$  of the particle distribution as a function of the Stokes number for  $R_\lambda = 460$  and various Froude numbers as labeled. Smaller Reynolds numbers (not shown here) display a similar behavior.

## $\mathcal{D}_2$ : What it tells us

- Gravity acts in a non-uniform manner.
- It tends to enhance concentration (decrease  $\mathcal{D}_2$ ) when both the Stokes and the Froude numbers have moderate values.
- When  $Fr \ll 1$ , clustering is decreased for  $St \lesssim 1$  and increased for  $St \gtrsim 1$ .
- For all finite  $Fr$ , one observes that  $\mathcal{D}_2$  saturates to a finite value when  $St \rightarrow \infty$ .
- For  $V_g \gg u_\eta$ , the fractal dimension  $\mathcal{D}_2$  is a function of the effective Stokes number  $\tilde{S}$  only, which for  $St \gg Fr$  becomes independent of  $St$ .
- In this asymptotics, the correlation dimension depends solely on  $Fr$ .
- The limiting value of  $\mathcal{D}_2$  is a non-monotonic function of  $Fr$ .



# Implication

- The increase in clustering observed for order-unity values of  $St$  and  $Fr$  means that settling can significantly impact the timescales of interaction between particles.
- When interested for instance in the collisions, estimations of the geometrical rate involve the probability density that two particles are at a distance  $r = 2a$  equal to the sum of their radii and thus scales as  $(2a)^{\mathcal{D}_2-1}$ .
- However, this quantity alone is not enough as the collision rate involves also the typical velocity at which particles approach each other.
- Indeed, for same-size particles, it is given by setting  $r = 2a$  in the approaching rate.

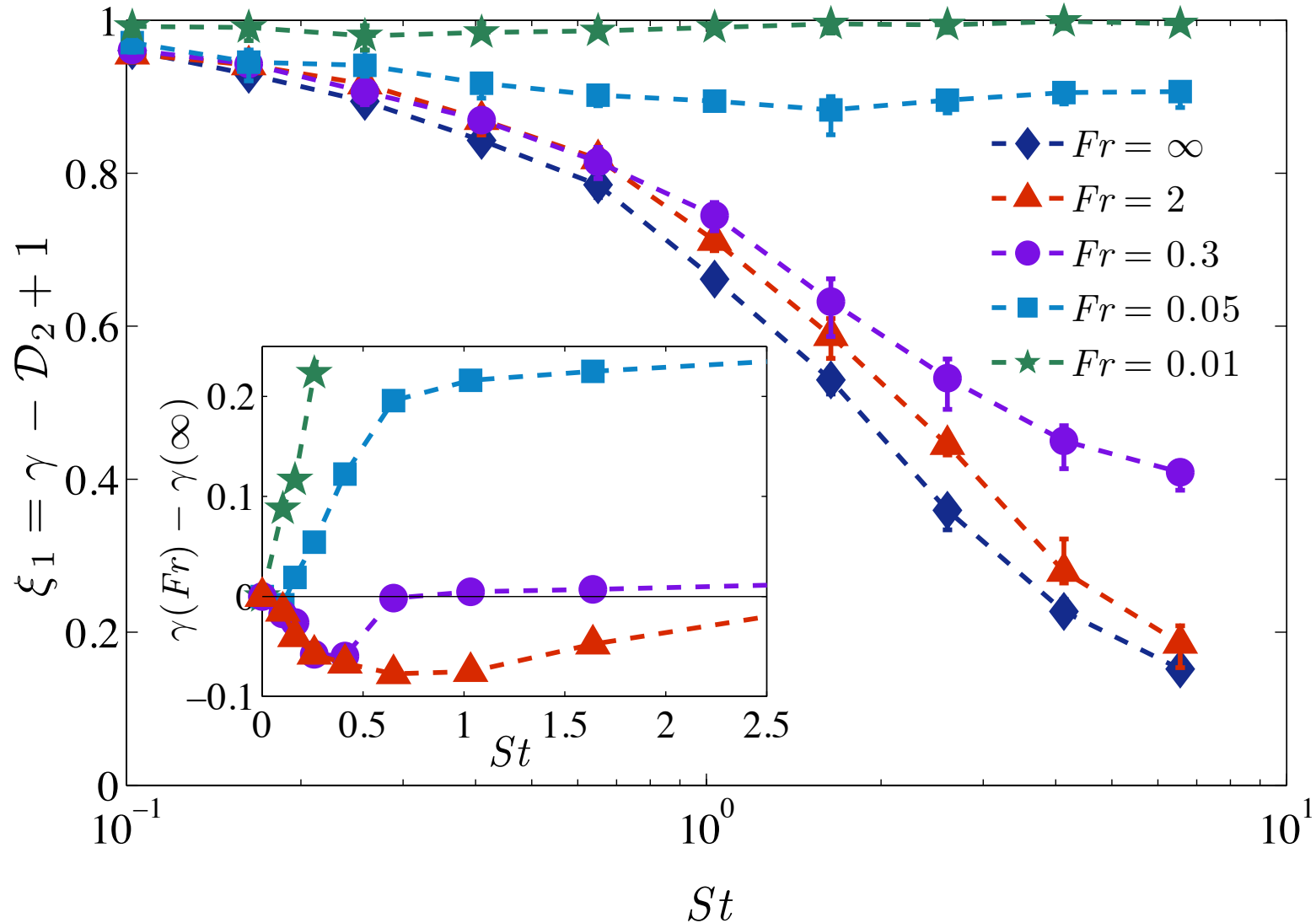
$$\kappa(r) = - \langle w \theta(-w) \delta(|\mathbf{R}| - r) \rangle ,$$

where  $w = d|\mathbf{R}|/dt$  is the longitudinal velocity difference between particles,  $\theta$  the Heaviside function, and  $\langle \cdot \rangle$  the average over all particle separations  $\mathbf{R}$ .

## The Approaching Rate

- $\kappa(r) = - \langle w \theta(-w) | |\mathbf{R}| = r \rangle (d\mathbb{P}_2/dr)$ , where  $w = d|\mathbf{R}|/dt$  is the longitudinal velocity difference between particles,  $\theta$  the Heaviside function, and  $\langle \cdot \rangle$  the average over all particle separations  $\mathbf{R}$
- This last quantity behaves also as a power of  $r$  for  $r \ll \eta$  with an exponent  $\xi_1$  given by the first-order structure function of particle velocities.
- This implies that  $\kappa(r) \sim r^\gamma$  with  $\gamma = \xi_1 + \mathcal{D}_2 - 1$ .
- The dependence of  $\gamma$  upon  $St$ , which encompasses particle clustering and velocity differences statistics, determines how the collision rate depends on the particles size and inertia.

# Approaching Rates



Exponent of the velocity difference  $\xi_1 = \gamma - \mathcal{D}_2 + 1$  as a function of the Stokes number for different  $Fr$  and  $R_\lambda = 460$ . Inset: difference between the approaching rate exponent  $\gamma$  associated to the different values of  $Fr$  and that associated to particles feeling no gravity ( $Fr = \infty$ ).

# Understanding Approaching Rates

- $\kappa(r) \sim r^\gamma$  with  $\gamma = \xi_1 + \mathcal{D}_2 - 1$ .
- For  $Fr = \infty$ ,  $\xi_1 = 1$  at small  $St$  (tracers) and  $\xi_1 = 0$  for  $St \rightarrow \infty$  (scale-independent velocity differences).
- When  $Fr$  decreases, the effective Stokes number decreases, so that particles get closer to tracers of the effective flow and  $\xi_1 \rightarrow 1$ .

M. Wilkinson, *et al.*, Phys. Rev. Lett. **97**, 048501 (2006).

J. Bec, *et al.*, J. Fluid Mech. **646**, 527 (2010).

J. Bec, *et al.*, Phys. Fluids **17**, 073301 (2005).

# Approaching Rates: Competing Mechanisms

- The two mechanisms determining the rate at which particles collide, namely preferential concentration and large velocity differences, are thus affected in a competing manner by gravity.
- The enhancement of particle clustering takes over the decrease of velocity differences when  $St \lesssim Fr$ .
- Hence,  $\gamma(Fr) < \gamma(\infty)$  for  $St \lesssim Fr$ , indicating that the collision rates between same-size particles are larger in the presence of gravity.
- These corrections are responsible for an important increase of the geometrical collision rate.
  - Example: In the settings of a highly-turbulent cloud, namely  $Fr = 0.3$  and  $St = 0.4$ , the collision rate doubles when the effect of gravity is included.

# Conclusions

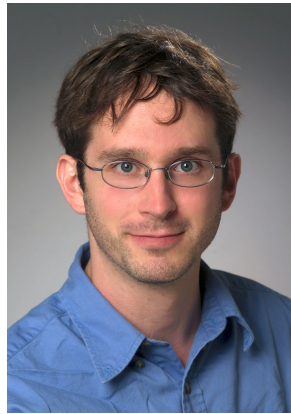
- Heavy particles suspended in a turbulent flow settle faster than in a still fluid.
- This effect stems from a preferential sampling of the regions where the fluid flows downward and is quantified as a function of the level of turbulence, of particle inertia, and of the ratio between gravity and turbulent accelerations.
- By using analytical methods and detailed numerical simulations, settling is shown to induce an effective horizontal two-dimensional dynamics that increases clustering and reduce relative velocities between particles.
- These two competing effects can either increase or decrease the geometrical collision rates between same-size particles and are crucial for realistic modeling of coalescing particles.

# Open Questions

- The functional form of the velocity difference PDF depends on the value of the Stokes number:
  - Extending arguments for synthetic flows and in the large  $St$  limit to moderate values of the Stokes numbers in real flows for which the contribution of inertial-range and dissipative-scale statistics cannot be neglected.
- The role of intermittency of turbulent velocity statistics and non-trivial Reynolds number dependencies of particle relative velocity and collision statistics.
- Coalescences.
- Modelling collision kernels.



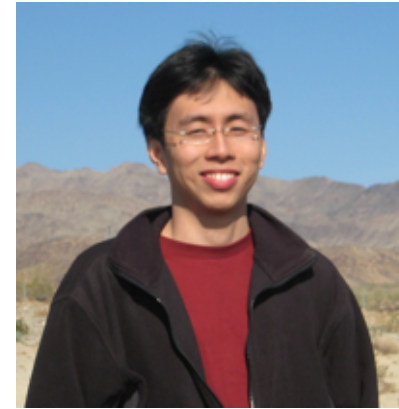
# Acknowledgements



**Gregory P. Bewley**



**Eberhard Bodenschatz**



**Ewe-Wei Saw**



**Holgar Homann**



**Jérémie Bec**

- The Indo–French Center for Applied Mathematics (IFCAM).
- The Airbus Group Corporate Foundation Chair in Mathematics of Complex Systems at the ICTS-TIFR and TIFR-CAM.
- European Research Council under the European Community's Seventh Framework Program (FP7/2007-2013, Grant Agreement no. 240579).
- IBM BlueGene/P computer JUGENE at the FZ Jülich through the PRACE project PRA031.

